ELSEVIER

International Journal of Pharmaceutics 243 (2002) 147–159

international journal of pharmaceutics

www.elsevier.com/locate/ijpharm

Polymorphic behavior of an NK1 receptor antagonist

Y. Wang *, R.M. Wenslow, J.A. McCauley, L.S. Crocker

Analytical Research Department, Merck Research Laboratories, R818-B112, P.O. Box 2000, Rahway, NJ 07065, USA

Received 1 April 2002; received in revised form 22 May 2002; accepted 22 May 2002

Abstract

Four anhydrous polymorphic forms (I, II, III and IV) of an NK1 receptor antagonist, Compound A, have been discovered. The pure compound can exist as either Forms I or II at room temperature and Forms III or IV at elevated temperatures. The four polymorphs were characterized by differential scanning calorimetry (DSC), thermogravimetric analysis, X-ray powder diffraction (XRPD) and solid-state NMR spectroscopy (SSNMR). Polymorphic transformations in the solid phase were studied using DSC, hot stage XRPD, temperature-modulated SSNMR and hot stage optical microscopy. The solubilities of Forms I and II in *tert*-butyl acetate at different temperatures were measured and the relative stability of the two forms was established. The thermodynamic transformation temperatures between Forms I and III, as well as Forms II and IV, were estimated by DSC. Transformation from Form III to IV, which is undetectable in a normal calorimetric run, was revealed through careful thermal programming. An interesting conversion route from Form I, a more stable form at room temperature, to Form II, a less stable form at room temperature was discovered.

Keywords: NK1 receptor antagonist; Polymorphism; Solid phase transformation; Differential scanning calorimetry; X-ray powder diffraction; Solid state NMR

1. Introduction

The tendency for organic compounds to crystallize in multiple crystal forms of the same pure substance is termed polymorphism, and the significance of this phenomenon in the pharmaceutical industry has been noted (Haleblian and McCrone, 1969; Haleblian, 1975). Once polymorphism is discovered for a drug candidate, the stabilities and transformation conditions for all polymorphic forms in the system must be investigated (Lord, 1988). Techniques such as hot stage microscopy, thermal analysis (TA), solution calorimetry, infrared spectroscopy, solubility measurements, density measurements, X-ray powder diffraction (XRPD), and X-ray single-crystal analysis have historically been available for the characterization of polymorphs (Threlfall, 1995). More recently, techniques such as solid-state NMR spectroscopy (SSNMR) have proven to be powerful tools for polymorphic investigations (Brittain, 1999; Bugay, 1993).

It has been well established that the thermodynamic stability as a function of temperature can

* Corresponding author. Tel.: +1-732-594-5803; fax: +1-732-594-3887

E-mail address: yaling_wang@merck.com (Y. Wang).

0378-5173/02/$ - see front matter
PII: S0378-5173(02)00292-2

be determined by the equilibrium solubilities of the individual polymorphs (Aguiar and Zelmer, 1969). Frequently, a linear relationship can be obtained by a van't Hoff plot over a relatively narrow temperature (Higuchi et al., 1963).

Polymorphic transformations are directed by the relative thermodynamic stabilities of the polymorphs if thermodynamic equilibria are achieved. However, kinetics plays an important role in real time, especially in the solid phase. Some studies on mechanisms of polymorphic transformations in molecular crystals have been reported (Byrn et al., 1999). Presumably, as in the primary crystallization process, the mechanisms of most solid–solid transformations involve the formation of critical nuclei of the new phase, followed by their growth (Dunitz and Bernstein, 1995). Solid-state transformations in molecular crystals often show a high degree of hysteresis. It may be necessary to heat the low-temperature form to a temperature well above the thermodynamic transformation temperature before signs of phase transformation can be detected. Even when no thermal event related to solid–solid transformation of the low-temperature form is detected below the melting point, this is not sufficient proof that the system is monotropic. The transformation may simply be too slow to be observed or not occur at all under the given conditions (Dunitz and Bernstein, 1995). The studies on the polymorphic behaviors of Compound A (Fig. 1), 1-(5-{[(2*R*,3*S*)-2-({(1*R*)-1-[3,5-Bis(trifluoromethyl)phenyl]ethyl}oxy)-3-(4-fluorophenyl)morpholin-4-yl]methyl}-2H-1,2,3-triazol-4-yl)-*N*,*N*-dimethylmethanamine hydrochloride, a high affinity, orally active, h-NK1 receptor antagonist (Harrison et al., 2001), are summarized in this paper. Two polymorphic forms of Compound A (Form I and II) have been observed at room temperature. Additional polymorphs (Form III and IV) were only observed at elevated temperatures.

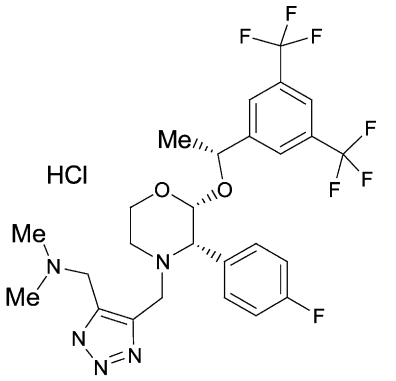

Fig. 1. Structure of Compound A.

In this study, the versatility of multiple techniques was demonstrated in providing a full characterization of the polymorph system of Compound A. Differential scanning calorimetry (DSC), XRPD, SSNMR and solubility studies were used to characterize crystal Forms I and II of Compound A and to assess their relative stability. DSC, hot stage XRPD and temperature-modulated SSNMR were used to identify two additional polymorphs (III and IV). In addition, temperature cycling experiments on DSC and hot stage XRPD revealed the transformation from Form III to IV, which is otherwise undetectable in a normal calorimetric run, and supported a hypothesis of an interesting phase transformation route from a more stable polymorph at room temperature (Form I) to a less stable polymorph at room temperature (Form II). Temperature cycling experiments by DSC were also successfully used to estimate the thermodynamic transformation temperature between Forms I and III, as well as Forms II and IV. The equilibrium solubilities of Forms I and II in *tert*-butyl acetate were measured and the van't Hoff plot was constructed. The relative stability of Forms I and II was established. Polymorphic transformations between Form I and III, as well as Form II and IV were also studied by optical microscopy.

2. Materials and methods

2.1. Materials

Compound A was prepared at Merck Research Laboratories, Rahway, NJ. *Tert*-butyl acetate (99 + %), used in solubility studies, was purchased from Aldrich.

2.2. Differential scanning calorimetry

Thermograms were acquired using a TA Instrument DSC 2910 differential scanning calorimeter. The experiments were run in an open pan with nitrogen flow. A pre-heating cycle, where the sample was heated at 10 °C/min from room temperature to 130 °C and then cooled down to room temperature, was implemented to remove the residual solvent. Calibration of temperature and cell constants were performed with indium under identical heating rates as used in sample analysis.

2.3. Thermogravimetric analysis

Thermogravimetric analyses (TGs) were conducted using a Perkin Elmer TGA 7 or Pyris 1 thermogravimetric analyzer. A heating rate of 10 °C/min was employed and a nitrogen purge was used. The balance was calibrated using a standard weight, and the sample temperature was calibrated using Curie-point standards.

2.4. X-ray powder diffraction

XRPD patterns were collected on a Philips Analytical X-ray instrument with a XRG 3100 generator and PW 3710 mpd controller. Copper K-Alpha 1 radiation at 45 KV, 40 mA was used. Samples were scanned between 2 and 40° (2θ) at 0.08°/s.

2.5. Hot stage X-ray powder diffraction

The X-ray instrument described above has a second goniometer, which is coupled with a TTK hot stage with TCU 100 Temperature Control Unit from Anton Paar. During the experiments, samples were heated at 10 °C/min to a desired temperature and held at that temperature while the XRPD data were collected. Subsequently the samples were either heated or cooled to another temperature for analysis. Samples were scanned between 5 and 35° (2θ) at 0.02°/s on the hot stage with a nitrogen gas purge.

2.6. Solid-state NMR spectroscopy

All $^{1}H/^{13}C$ Cross-Polarization Magic-Angle Spinning (CP/MAS NMR) spectra were obtained on a Bruker DSX-400 NMR spectrometer (9.4 T magnetic field strength) using a Bruker double-resonance CP/MAS probe with variable temperature capabilities and a standard CP/MAS pulse sequence. The ^{13}C and ^{1}H resonance frequencies are 100.627 and 400.136 MHz respectively at this magnetic field strength. $^{1}H/^{13}C$ CP/MAS NMR experiments were performed with 2.0 ms contact times, 4 k of data points were acquired in 60 ms and then zero-filled to 8 k before transformation using 20.0 Hz of line broadening. Between 64 and 256 scans were acquired. Recycle delays for the $^{1}H/^{13}C$ CP/MAS NMR experiments were 7.0 s. Rotor frequency was 7.0 kHz. All ^{13}C spectra were referenced to TMS using the carbonyl carbon of glycine (176.03 ppm) as a secondary reference.

2.7. Solubility measurement

A solid sample was suspended in solvent in a sealed glass tube and agitated in a temperature controlled water bath for a period of time. After the equilibration, the solid was allowed to settle by rapid centrifugation, the glass tube was then opened and the supernatant was filtered into a pre-weighed volumetric flask (when performing solubility measurements at elevated temperatures, the pipet and syringe with filter attached were pre-warmed). The flask with solution was weighed and the concentration of the supernatant was determined by HPLC. The solubility was then calculated. Experiments were performed in triplicate and the results averaged.

2.8. Hot stage optical microscopy

The hot stage optical microscopy was conducted on a Leica DMRP microscope, equipped with a Polaroid DMC—2 camera and a hot stage with 50/70—600 Controller by Creative Devices, Inc. Image-Pro Plus by Media Cybernetics was used to process the data.

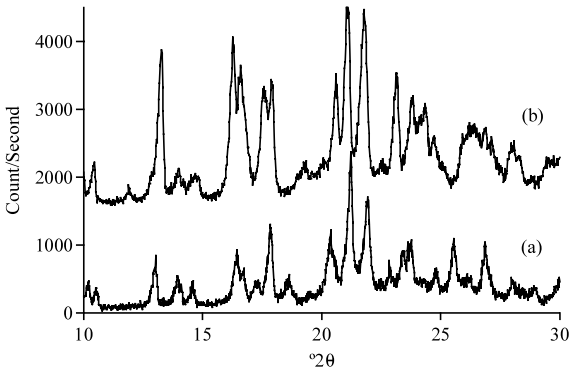

Fig. 2. XRPD patterns. (a) Form I, (b) Form II.

3. Results and discussion

3.1. Discovery and characterization of Forms I–IV

Adding *n*-heptane to a solution of Compound A in a mixture of ethyl acetate and iso-propanol (9/1 volume ratio) yields either Form I or II depending on the concentration and rate of addition of the anti-solvent. For example, slow addition of anti-solvent into a saturated solution of Compound A will result in pure Form I. On the other hand, rapidly pouring anti-solvent into a saturated solution of Compound A will result in Form II. XRPD patterns and SSNMR spectra obtained for both Forms I and II are shown in Fig. 2 and Fig. 3, respectively. The NMR spectrum for Form II displays clear distinctions compared to Form I especially in the region around 23 ppm which can be attributed to either conformation changes or packing differences. A 0.2% weight loss, significantly less than any stoichiometric amount, due to residual solvents was observed by TG for each form implying that no solvation occurred.

The DSC curve at 10 °C/min of Form I is shown in Fig. 4a. Two endotherms were observed at extrapolated onset temperatures (T_{ons}) of 108.0 °C ($\Delta H = 4.0$ J/g) and 200.1 °C ($\Delta H = 46.3$ J/g), respectively. The second endotherm is at-

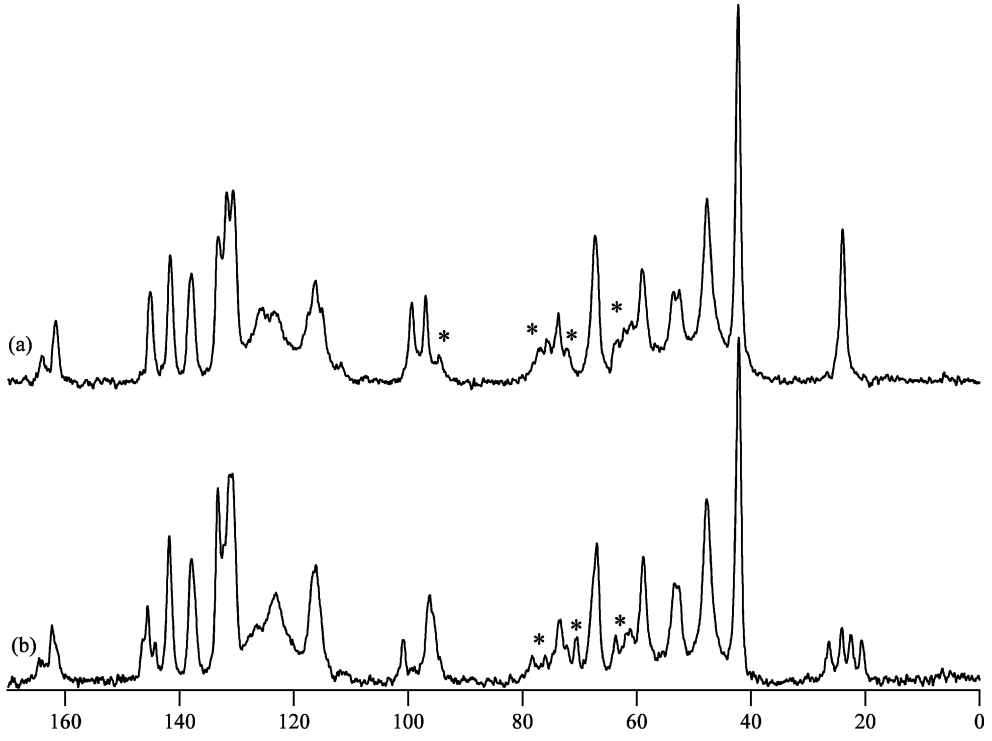

Fig. 3. Ambient temperature carbon CP/MAS Solid-State NMR spectra. (a) Form I, (b) Form II (* represent spinning sidebands).

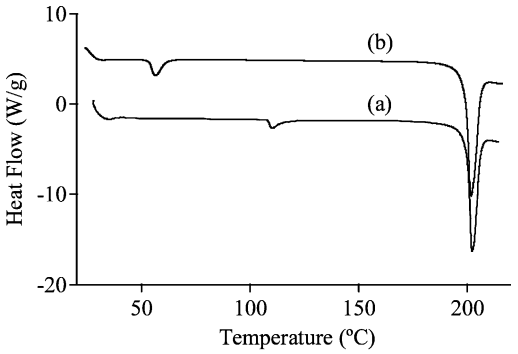

Fig. 4. DSC scan at 10 °C/min. (a) Form I, (b) Form II.

tributed to the melting with decomposition of the sample. In order to investigate the first endotherm, the sample was analyzed by hot stage XRPD and temperature-modulated SSNMR. Fig. 5a shows the XRPD pattern of the sample at 140 °C. The pattern is clearly different from that of Form I or II (the goniometer coupled with the hot stage produces reduced signal intensity compared to the goniometer used at ambient conditions, for example, Fig. 2). Additionally, SSNMR displayed a new spectrum at 115 °C on a Form I sample (Fig. 6). The primary SSNMR differences between Form I and III include doublets at ~ 100 and ~ 48 ppm in Form I collapsing to singlets for Form III. This may indicate less molecules in the asymmetric unit cell for Form III compared to Form I. An additional significant peak shift occurs for the peak at 73 ppm in Form I shifting to 78 ppm in Form III. The same XRPD pattern

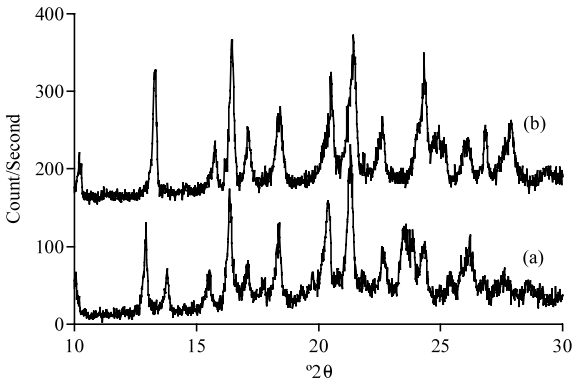

Fig. 5. XRPD pattern. (a) Form III, (b) Form IV.

and SSNMR spectrum as those of Form I were observed after the samples were cooled to room temperature in above experiments respectively, indicating no chemical decomposition involved. Therefore, the first endotherm on the DSC curve of Form I is due to the polymorph transformation from Form I to a new form, Form III. Form III converts back to Form I upon cooling based on DSC, XRPD, and SSNMR. It is evident that Form I and III are enantiotropic polymorphs. Rapid cooling, even quenching with ice–water, failed to obtain Form III at room temperature, suggesting a low activation energy barrier between these two forms. To estimate the thermodynamic transformation temperature between Forms I and III by DSC, a Form I sample was cycled around the transformation temperature, between 20 and 130 °C at 0.5 °C/min (Fig. 7). An endotherm with T_{ons} of 106.9 °C was observed upon heating and an exotherm with T_{ons} of 101.3 °C was observed upon cooling. The difference between the heating and cooling T_{ons} is attributed to hysteresis, commonly observed for solid phase transformations (Dunitz and Bernstein, 1995). The true thermodynamic transformation temperature between Forms I and III lies between 101.3 and 106.9 °C and can be estimated as the mean of the two values $\pm$ the spread (104 ± 3 °C).

The DSC curve at 10 °C/min of Form II is shown in Fig. 4b. Two endotherms were observed at T_{ons}'s of 53.3 °C ($\Delta H = 6.1$ J/g) and 199.4 °C ($\Delta H = 47.0$ J/g) respectively. Again, the second endotherm is attributed to the melting with decomposition of the sample. Hot stage XRPD and SSNMR were again used to study the structural significance of the first endotherm. Fig. 5b displays the XRPD pattern of the sample at 80 °C. The powder pattern is different from that of Form I, II or III. A new spectrum was also observed at 80 °C by SSNMR (Fig. 8). The main SSNMR spectral differences between Form III and IV include peaks at 23.3, 76.6, and 99.3 ppm in the Form III spectrum being shifted to 23.6, 77.2, and 99.7 ppm respectively in the Form IV spectrum. The reversibility of XRPD pattern and SSNMR spectrum between room temperature and 80 °C was observed and indicates no chemical decomposition. Therefore the first endotherm is

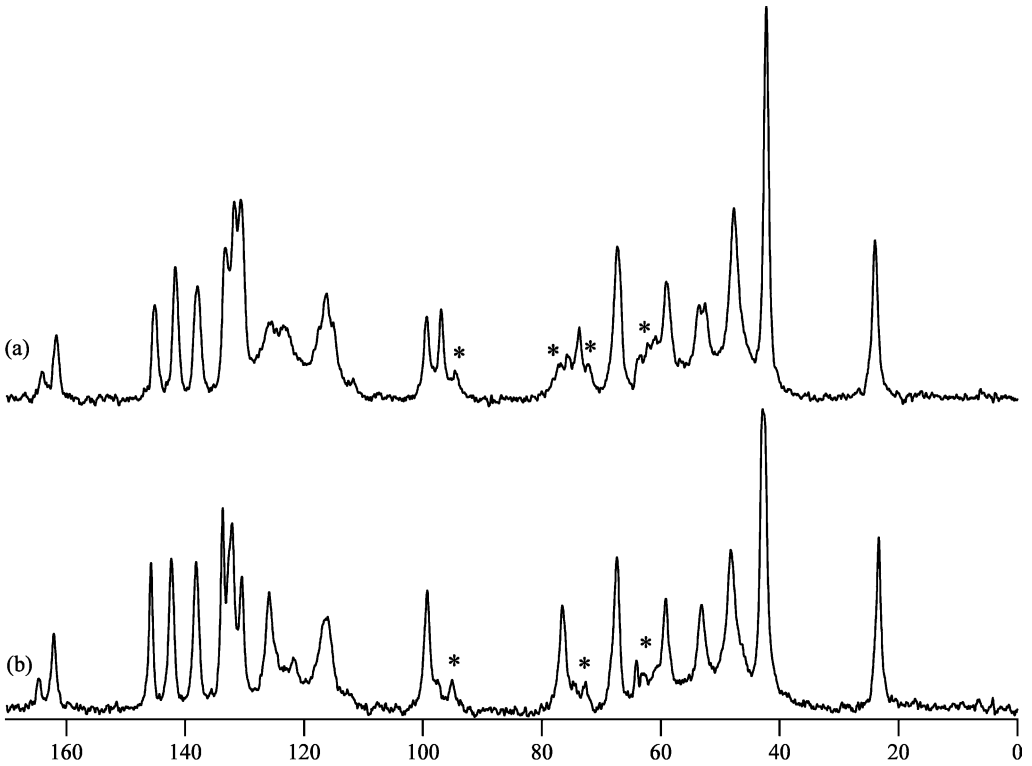

Fig. 6. Carbon CP/MAS solid-state NMR spectra. (a) Form I, (b) Form III (* represent spinning sidebands).

attributed to transformation of Form II to another new form, Form IV. Form IV converts to Form II readily upon cooling, again suggesting low activation energy barrier between these two forms. As was the case for Form I and III, Form II and IV are also enantiotropic polymorphs. Temperature cycling experiment at 0.5 °C/min on DSC suggested a thermodynamic transformation temperature of 51 ± 3 °C.

It is remarkable that there seem to be two families of polymorphs. Forms I and III belong to the first family (family 1) and Forms II and IV belong to the second (family 2). Within the same family, the two members transform freely at the transformation temperature.

3.2. Assessing the relative stabilities of Form I and II

In order to establish the thermodynamic stability relationship as a function of temperature between Forms I and II, solubilities of these two forms in *tert*-butyl acetate at various temperatures were measured (Table 1). The presence of the starting form after equilibration was confirmed by XRPD on the remaining solids. Making the approximation that solubilities may be used in

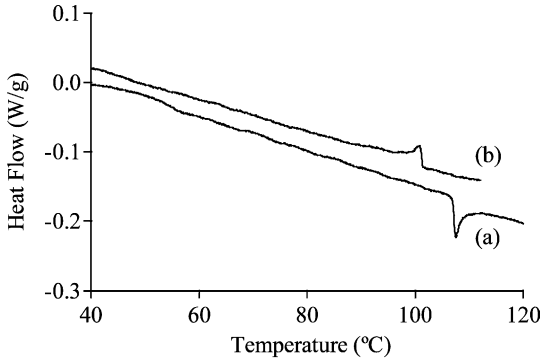

Fig. 7. DSC scan of Form I at 0.5 °C/min. (a) Heating, (b) cooling.

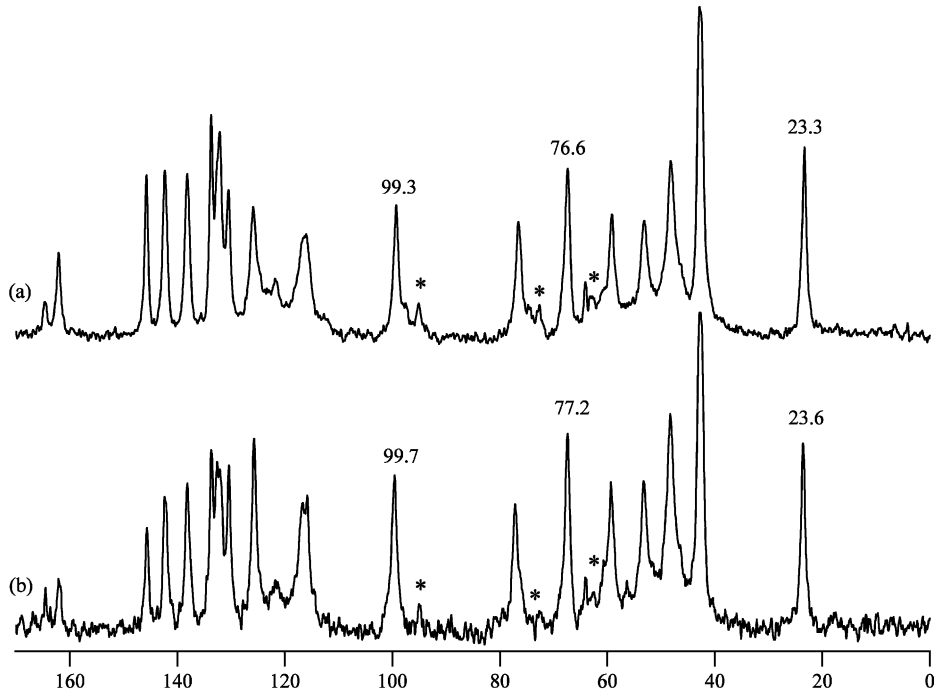

Fig. 8. Carbon CP/MAS solid-state NMR spectra for (a) Form III and (b) Form IV (* represent spinning sidebands).

place of the activities (Ghodbane and McCauley, 1990), the van't Hoff plot was constructed (Fig. 9). Form I has lower solubility than Form II over the entire temperature range of the measurements, signifying that Form I is the more thermodynamically stable form. Extrapolation of the linear least-squares-derived lines predicts a reversal of the thermodynamic stability at a temperature of 129 °C. This temperature is higher than the transition temperatures between Forms I and III, and Forms II and IV, which explains the absence of direct conversion from Form I to II.

3.3. Discovery of an interesting solid phase transformation route from Form I to II

From the discussion above, the melting endotherm on the DSC curves of Form I and II may be attributed to the melting of Form III and IV respectively. However, by comparing the melting endotherms, it is evident that both the melting temperature and the heat of fusion of a Form I sample are the same as those of a Form II sample within experimental error. If these endotherms represent the melting of Form III and IV, the enthalpy (therefore entropy) of Form III and IV at their melting temperatures are too similar to be differentiated by the instrument used in this study. Another hypothesis to explain the DSC data is that a phase transformation (undetectable by this DSC instrument) occurred before melting so that the two melting endotherms are actually caused by the melting of the same solid phase. Tempera-

Table 1
Solubilities of Compound A polymorphs in *tert*-butyl acetate

Temperature (°C)	Form I (mg/g solvent)	Form II (mg/g solvent)
15.3	1.33 (0.05)	2.3 (0.2)
25.0	2.01 (0.09)	2.64 (0.08)
35.3	2.3 (0.1)	3.4[a] (0.1)
39.3		3.89[a] (0.07)
65.0	4.82 (0.07)	

$n = 3$ unless specified, standard deviation in parentheses.
[a] $n = 2$.

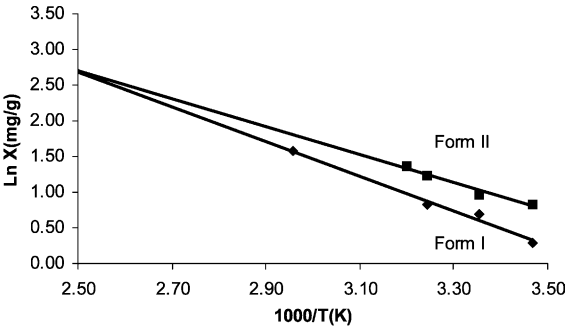

Fig. 9. van't Hoff plot of Form I and II in *tert*-butyl acetate.

ture cycling experiments by DSC were conducted to provide insight into this postulate. A sample of Form I was heated at 10 °C/min on the DSC to 183 °C (Fig. 10a), then cooled down to room temperature (the sample at this point will be referred to as Sample X, in order to differentiate it from the starting material). Sample X is heated to 220 °C (Fig. 10b). One endotherm at T_{ons} of 106.9 °C was observed on the first heating pass, indicating the starting material was pure Form I. However, two endotherms at T_{ons}'s of 54.1 °C ($\Delta H = 5.9$ J/g) and 104.7 °C ($\Delta H = 0.3$ J/g) were observed on the heating pass for Sample X. These two endotherms are characteristic transformation endotherms from Form II to IV and Form I to III respectively, indicating that Sample X contains both Form I and II. Based on the heat of transformation of Sample X and those of pure Form I and II, it is obvious that Sample X is

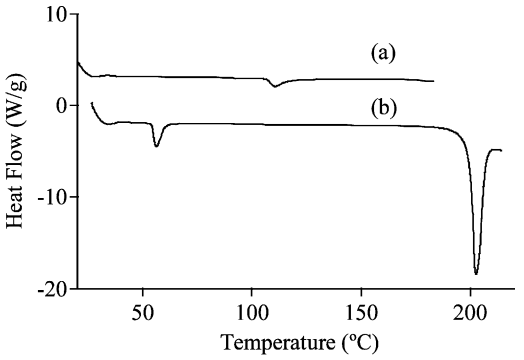

Fig. 10. DSC scans of Form I. (a) 1st heating pass, (b) 2nd heating pass.

composed primarily of Form II. This indicates that a large amount of Form I in the original sample has converted to Form II during the cycling experiment. The DSC work outlined above led to the hypothesis for the phase transformations of Compound A: Form I converted to III upon heating, and at higher temperature Form III converted to Form IV, and then upon cooling, Form IV converted to II. This hypothesis was confirmed by hot stage XRPD. Fig. 11 shows the XRPD patterns of a Form I sample taken at 25, 140, 180 and 25 °C (cooled down from 180 °C). The four individual patterns match Forms I, III, IV and II respectively. Higher temperatures had to be applied (compared to DSC data) to observe transformations from I to III and III to IV due to the temperature gradient between the bottom of the sample and the top, as well as the slow transformation rate from Forms III to IV in the latter case. This slow transformation may explain the lack of an observable thermal event directly related to the transformation of Form III to IV in the DSC scan of Form I (Fig. 4a).

In order to investigate the lowest temperature required to observe transformation from Form III to IV, additional temperature cycling experiments were conducted (see Fig. 12 for the temperature program). Form I was heated at 0.5 °C/min to temperature T, then cooled to 20 °C at the same rate. The 0.5 °C/min heating rate was applied to allow enough time for the possible transformation. The 0.5 °C/min cooling rate was used to allow the cell temperature to catch up since no cooling system was connected during the experiments. The sample was then heated at 10 °C/min to 130 °C and then cooled to 20 °C at 0.5 °C/min. The 10 °C/min heating step was inserted because the sensitivity of DSC analysis at 10 °C/min is much higher than at 0.5 °C/min. The same cycle was repeated another two times with different T's. T equaled 130, 135 and 140 °C respectively for the first, second and third cycle, respectively. At the last cycle, the sample was heated to 220 °C at 10 °C/min and the run was ended.

Fig. 13a–c displayed the DSC traces collected during the first, second and third heating passes

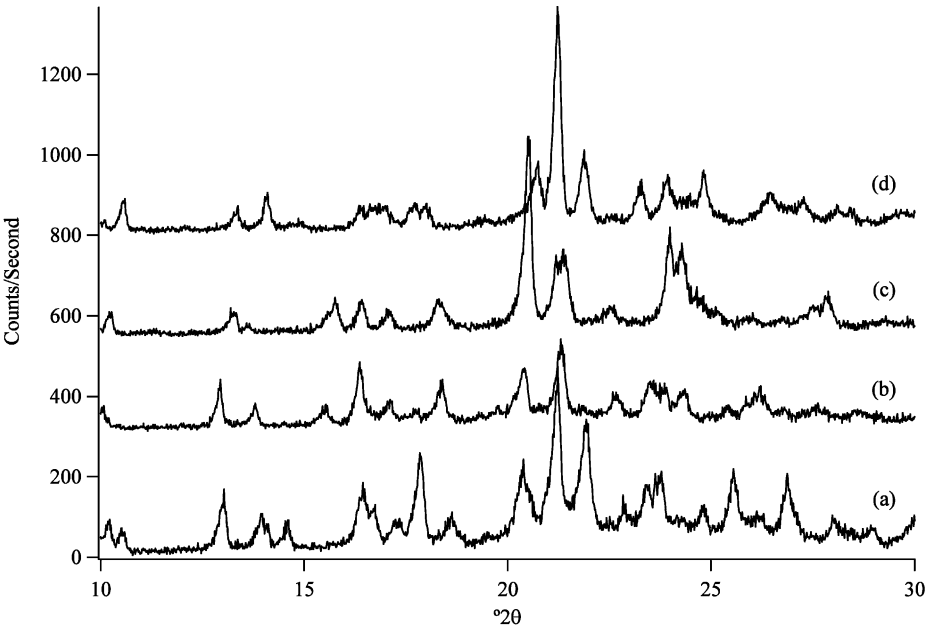

Fig. 11. XRPD patterns. (a) Room temperature, (b) 140 °C, (c) 180 °C, (d) room temperature (cooled down from 180 °C).

at 10 °C/min. Form II was detected on the second and the third passes based on the evidence that an endotherm at T_{ons} of 52.4 °C was observed on each pass. The results showed that the phase transformation from Form III to IV can occur when $T \geqslant T_{III}$, where 130 °C $< T_{III} <$ 135 °C. Approximately 7% of the sample had converted to Form II at room temperature after the second cycle, indicating a very slow transformation from Form III to IV at 135 °C.

3.4. Polymorph map

Having identified four polymorphs and studied their transformation, a polymorph map (Fig. 14) may be used to illustrate the relationships among these polymorphs. As discussed before, the four polymorphs can be divided into two families. Forms I and III belong to family 1 and Forms II and IV belong to family 2. Within the same family, the two members transform freely at the transformation temperature. However, only relatively slow transformation was observed between the two families.

3.5. Optical microscopy of polymorphic transformations

A Form II sample contained between two glass slides was heated at 2 °C/min on the hot stage mounted on a microscope, and then cooled to room temperature after heating to 80 °C. Crossed polars were placed between the light source and the sample. Fig. 15a shows a picture taken at room temperature. During heating, no change was observed between room temperature and

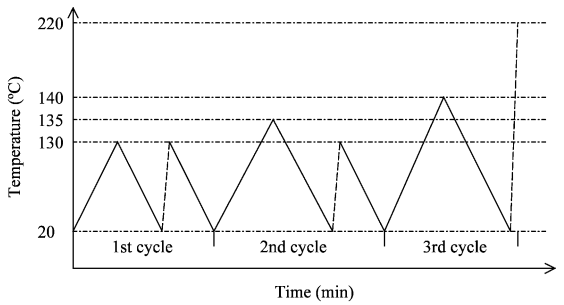

Fig. 12. Temperature program used for temperature cycling experiments on DSC. *Solid line:* 0.5 °C/min, *dashed line:* 10 °C/min.

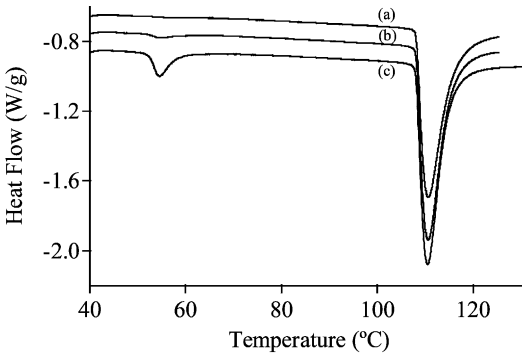

Fig. 13. DSC scans at 10 °C/min from temperature cycling experiments on DSC. (a) 1st pass, (b) 2nd pass, (c), 3rd pass.

58 °C. Between 59 and 62 °C, apparent motion of the particles was observed in some spots. Changes ceased above 62 °C. Some of the changes can be recognized in the spots pointed by the arrows in Fig. 15b (taken at 65 °C) when compared to the same spots in Fig. 15a. Apparently, the observed phenomena corresponded to the transformation from Form II to IV. The apparent motion was not likely due to the physical movement of the particles, but caused by molecular rearrangements within the particles. The rearrangements changed the interaction between the crystals and the polarized light and therefore the appearance of the particles. Apparently the molecular rearrangement should occur through the entire sample. Some areas have less observable changes than others because most of the particles are agglomerates of fine particles. Fig. 15c displays a picture taken after above sample was cooled to room temperature after the heating. The image has returned to its appearance in Fig. 15a, indicating a reversible transformation. This agrees with the earlier discussion about the transformation between Form II and IV.

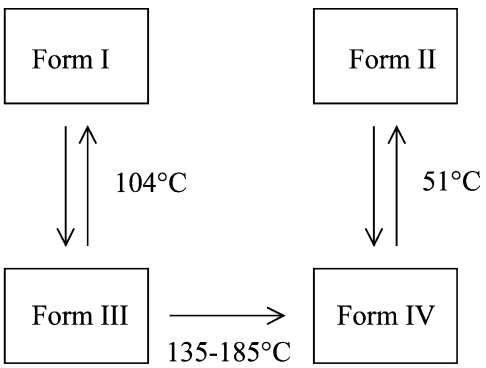

Fig. 14. Polymorph map of Compound A.

During the transformation between Form II and IV, no isotropic phase was observed by microscopy. This suggests that the formation of critical nuclei of the new phase and their growth occurred in the old phase. In other words, no disordered intermediate phase was involved in the transformation. The fact that Fig. 15c looked exactly like Fig. 15a also suggests the molecules had memories of their alignments.

A Form I sample was also studied by hot stage microscopy. Fig. 16 shows the pictures taken at room temperature, 125 °C, and room temperature again (cooled down from 130 °C). No change was detected during transformation between Form I and III, which may suggest that a lower degree of molecular rearrangement was involved during the transformation.

3.6. Kinetic aspect of solid phase transformation

Forms II and IV interconvert easily by increasing or decreasing the temperature. However, the evidence shows that Forms II and IV are metastable with respect to Form I over the temperature range in which Forms II and IV interconvert. Therefore, greater kinetic barriers must exist for the transformations between Forms II and I, and IV and I, than between Forms II and IV. Forms I and III also interconvert easily. The easily interconverting polymorphs may be called families, and since Forms I and III are members of a different family than Forms II and IV, it is reasonable to predict that the interconversion of Form III and IV would be relatively slow, which is what is observed. These kinetic effects make it possible for the more stable form at room temperature, Form I, to be converted to a less stable form at room temperature, Form II, through a series of temperature manipulations. Solving the structures of the four polymorphs by X-ray single-crystal diffraction and powder diffraction is in progress and will provide insight into the mechanisms of transformations among the four polymorphic forms.

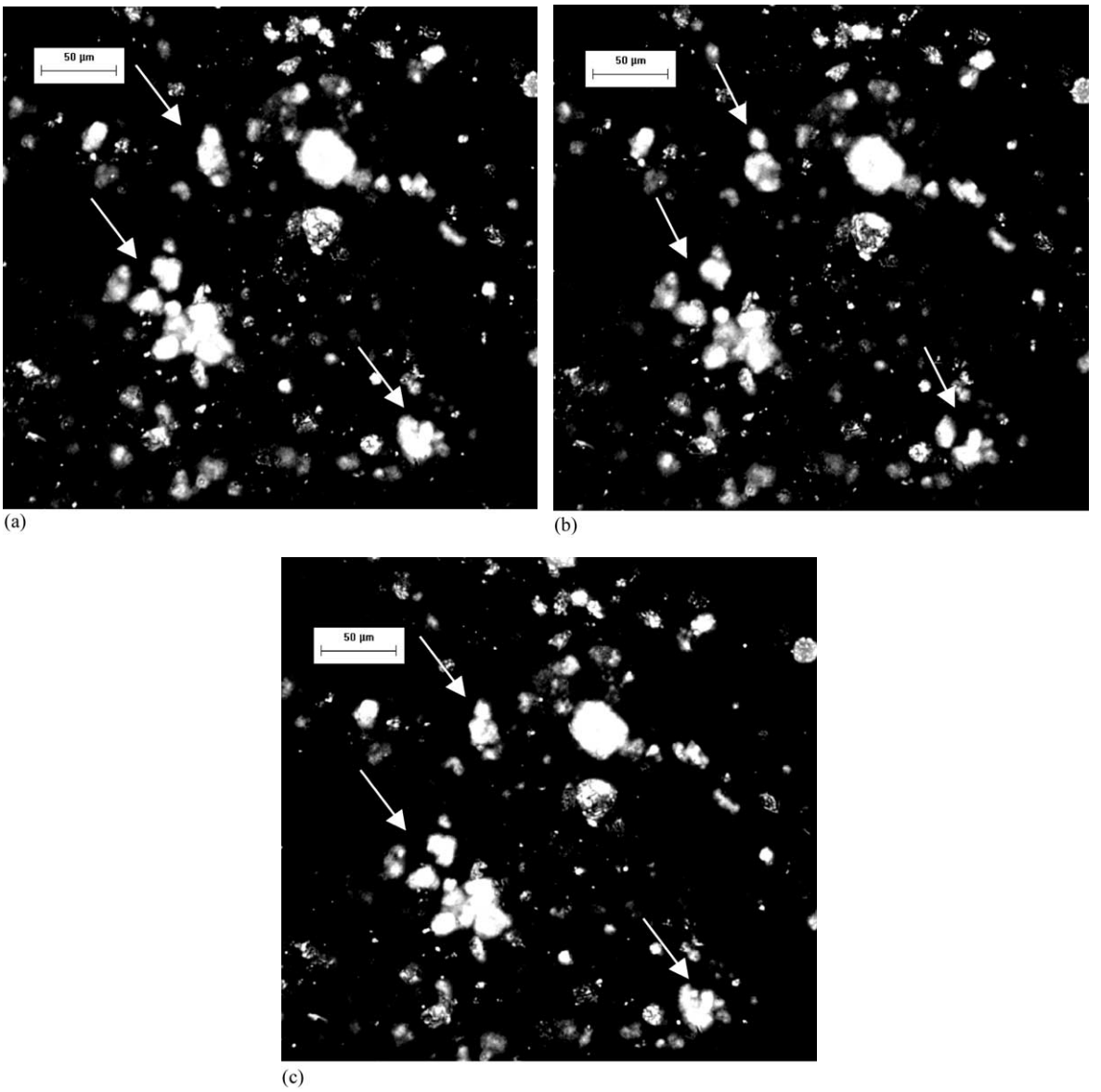

(a) (b) (c)

Fig. 15. Hot stage microscopy of Form II. (a) Room temperature, (b) 65 °C, (c) room temperature (cooled down from 80 °C).

4. Conclusions

Four polymorphic forms of Compound A were identified and a polymorph map was constructed. Forms I and II were obtained at room temperature, Forms III and IV exist only at elevated temperatures. Form I is thermodynamically more stable than Form II based on their equilibrium solubilities. The four polymorphs can be divided into two families. Form I and III belong to family I and Forms II and IV belong to family 2. Within the same family, the two members transform freely at the transformation temperature, implying low activation energy. Relatively slow transformation was observed between the two families, suggesting greater kinetic barriers. These kinetic effects make it possible for Form I, the more stable form at room temperature, to be converted

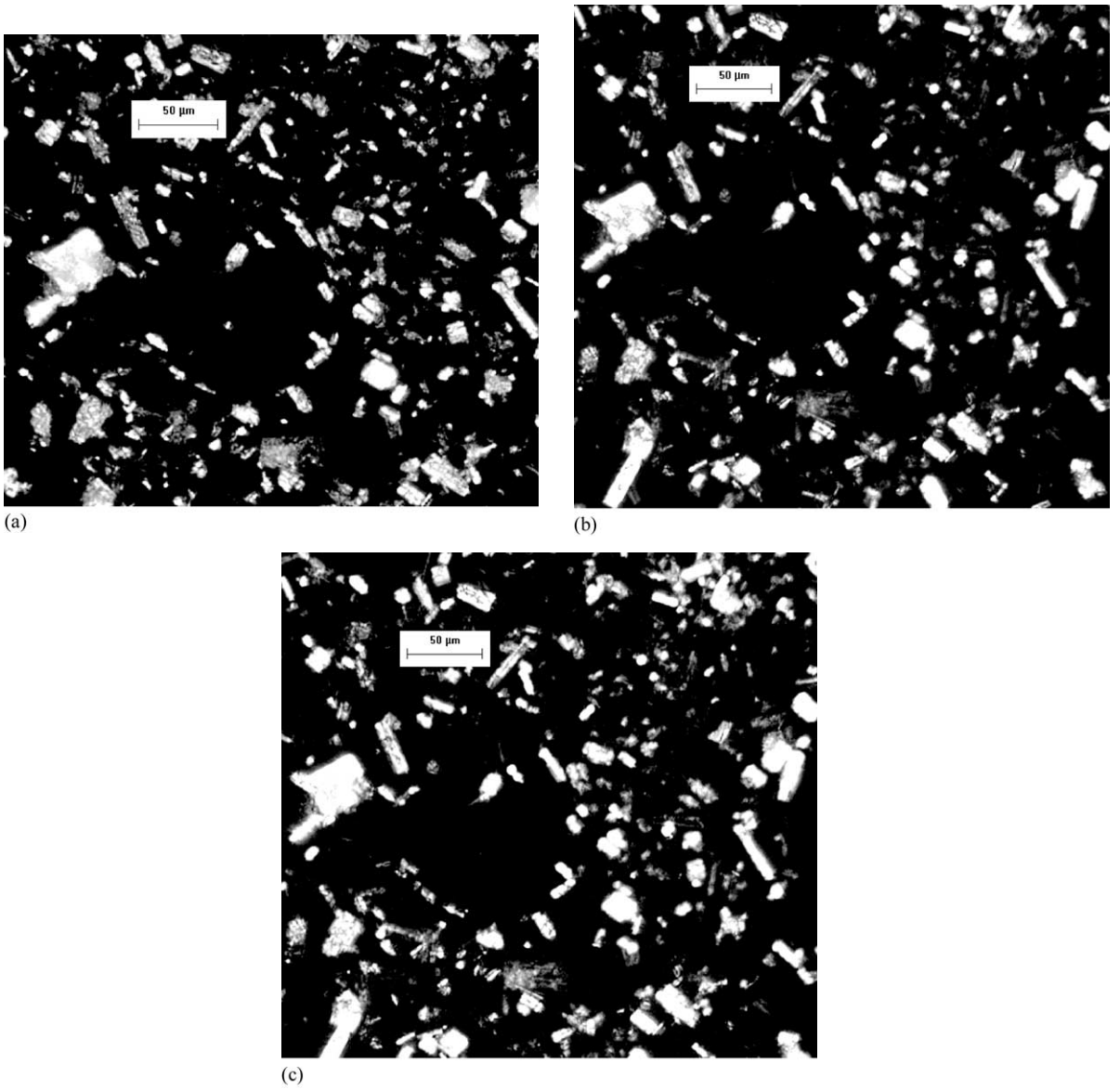

Fig. 16. Hot stage microscopy of Form I. (a) Room temperature, (b) 125 °C, (c) room temperature (cooled down from 130 °C).

to Form II, a less stable form at room temperature through temperature manipulations.

References

Aguiar, A.J., Zelmer, J.E., 1969. Dissolution behavior of polymorphs of chloramphenicol palmitate and mefenamic acid. J. Pharm. Sci. 58, 983–987.

Brittain, H.G. (Ed.), 1999. Polymorphism in Pharmaceutical Solids. Marcel Decker, New York, pp. 264–270.

Bugay, D., 1993. Solid-state nuclear magnetic resonance spectroscopy: theory and pharmaceutical applications. Pharm. Res. 10, 317–332.

Byrn, S.R., Pfeiffer, R.R., Stowell, J.G., 1999. Solid-State Chemistry of Drugs, second ed., 259–277.

Dunitz, J.D., Bernstein, J., 1995. Acc. Chem. Res. 28, 193–200.

Ghodbane, S., McCauley, J.A., 1990. Study of the polymorphism of 3-((3-(2-(7-chloro-2-quinolinyl)-(*E*)-ethenyl)-phenyl)((3-(dimethylamino-3-oxopropyl)thio)methyl)-thio)-propanoic acid (MK571) by DSC, TG, XRPD and solubility measurements. Int. J. Pharm. 59, 281–286.

Haleblian, J.K., 1975. Characterization of habits and crystalline modification of solids and their pharmaceutical applications. J. Pharm. Sci. 64, 1269–1288.

Haleblian, J.K., McCrone, W.J., 1969. Pharmaceutical applications of drugs. J. Pharm. Sci. 58, 911–929.

Harrison, T., Owens, A.P., Williams, B.J., Swain, C.J., Williams, A., Carlson, E.J., Rycroft, W., Tattersall, F.D., Cascieri, M.A., Chicchi, G.G., Sadowski, S., Rupniak, N.M.J., Hargreaves, R.J., 2001. An orally active, water-soluble neurokinin-1 receptor antagonist suitable for both intravenous and oral clinical administration. J. Med. Chem. 44, 4296–4299.

Higuchi, W.I., Lau, P.K., Higuchi, T., Shell, J.W., 1963. Polymorphism and drug availability. J. Pham. Sci. 52, 150–153.

Lord, A.G., 1988. BPC's and cGMP's. Pharm. Eng. 8, 30–35.

Threlfall, T.L., 1995. Analysis of organic polymorphs. Analyst 120, 2435–2460.